Density Functional Calculations of the ^{29}Si and ^{27}Al MAS NMR Spectra of the Zeolite Mazzite: Analysis of Geometrical and Electronic Effects

G. Valerio and A. Goursot*

UMR 5618 CNRS, Ecole Nationale Supérieure de Chimie, 8 rue de l'Ecole Normale, 34296 Montpellier, Cédex 5, France

Received: July 22, 1998; In Final Form: October 16, 1998

The ^{29}Si and ^{29}Al NMR chemical shifts of the two crystallographic sites of the zeolite mazzite have been evaluated from the NMR shielding tensors calculated using the SOS-DFPT method. The calculations were carried out on one-site and two-site models, including from one to three coordination shells around each site. The effects of the cluster size, basis set extension, and choice of the exchange and correlation functional have been analyzed. The 1T models including two coordination shells around the site are sufficient for a good description of the NMR peak separation, whereas the absolute values of the ^{29}Si and ^{29}Al NMR chemical shifts are obtained using a 2T model including the four-membered ring between the two sites. The effect of geometrical and electronic factors on the NMR chemical shifts have been analyzed, showing their dependence on the cluster size and also on the shape of the zeolitic system.

I. Introduction

Physical and chemical properties of zeolites, such as adsorption of molecules, cation exchange and catalysis are unambiguously related to their structure, i.e., the framework geometry, the nature and distribution of aluminum sites, and associated counterions.

Conventional techniques such as X-ray diffraction cannot fully describe all structural characteristics, in particular the topology of the aluminum distribution and the related local geometry.

The development of high-resolution solid-state NMR techniques, such as magic-angle spinning (MAS), has provided increased understanding of the zeolite chemistry. Indeed, ^{29}Si and ^{27}Al MAS NMR have become powerful tools for zeolite characterization. Moreover, ^{13}C and ^{1}H in situ NMR spectra are now used to study chemical reactions involving Bronsted acid sites.

^{29}Si MAS NMR spectra of zeolite materials show multiple signals which can be used to characterize the lattice structure. Their number and relative positions are indeed directly correlated with the local environment of each tetrahedral Si site (T), i.e., its crystallographic structure and the number of T′ substituents in the next shells. In highly siliceous materials, small structural differences, induced by crystallographically inequivalent environments of the silicon sites, can be detected, as was first demonstrated for silicalite by Fyfe et al.[1,2]

Substitution of Si by other elements such as Al, Ga, etc., leads to modified ^{29}Si NMR spectra. These spectral changes are correlated with the modifications of the framework geometry and also with electronic effects of the neighboring T′ sites. ^{29}Si MAS NMR spectra of zeolites with various Si/Al ratios have been used to determine the ordering of Si and Al atoms in the framework.[3−5] Empirical formulas have been derived which relate the substitution around the lattice sites and the corresponding chemical shifts δ (Si).[3,6] Empirical expressions relating the local structure around a site (TT distances, TOT angles) and its chemical shift have been used for various zeolitic systems.[7,11]

In all cases, including solids containing other elements than silicon, a general linear relationship has been found between δ (Si) and the average SiT distance or ⟨TOT⟩ angle, with the trend that the largest distance (angle) is related to the most negative δ (Si) (with respect to tetramethylsilane (TMS)). However, as expected, similar ⟨SiOSi⟩ and ⟨SiOAl⟩ angles do not correspond to the same δ(Si), showing that the substitution of Si by Al (or Ga, Ti, etc.) affects the neighboring Si through both geometric and electronic effects.

Several proposals have been made in the literature to explain the variation of δ (Si) in terms of electronic effects induced by the neighboring O and T atoms, such as the charge on the T element and the change of oxygen hybridization.[11,12]

To go beyond empirical analyses, interpretation and prediction of NMR spectra, an accurate approach is necessary. Provided that the models used for the zeolite sites are valid, the experimental NMR spectrum can be described and a correlation between the NMR parameters and the electronic structure of the system can be attempted. To this end, we have chosen to study the ^{29}Si and ^{27}Al spectrum of mazzite, which is a relatively simple zeolite with only two crystallographic sites. Using a density functional theory (DFT)-based methodology,[13] we have calculated the NMR shielding constants of the Si sites and models in which each T site in turn is replaced by aluminum. We have analyzed the effect of the cluster size and basis set extension on the evaluation of the NMR parameters. Finally, we have studied the effect of both geometrical and electronic factors on the calculated shielding constants.

II. Models

The framework of the natural zeolite mazzite and of its synthetic equivalent zeolite omega contains two nonequivalent crystallographic sites, that we will call T_I and T_{II}. In our calculations, we considered the experimental structure reported by Galli,[14] which corresponds to a solid with a Si/Al ratio of 2.7. In this context, we have chosen to compare the calculated ^{29}Si chemical shifts with the experimental spectra of mazzite

10.1021/jp983121i CCC: $18.00
Published on Web 12/19/1998

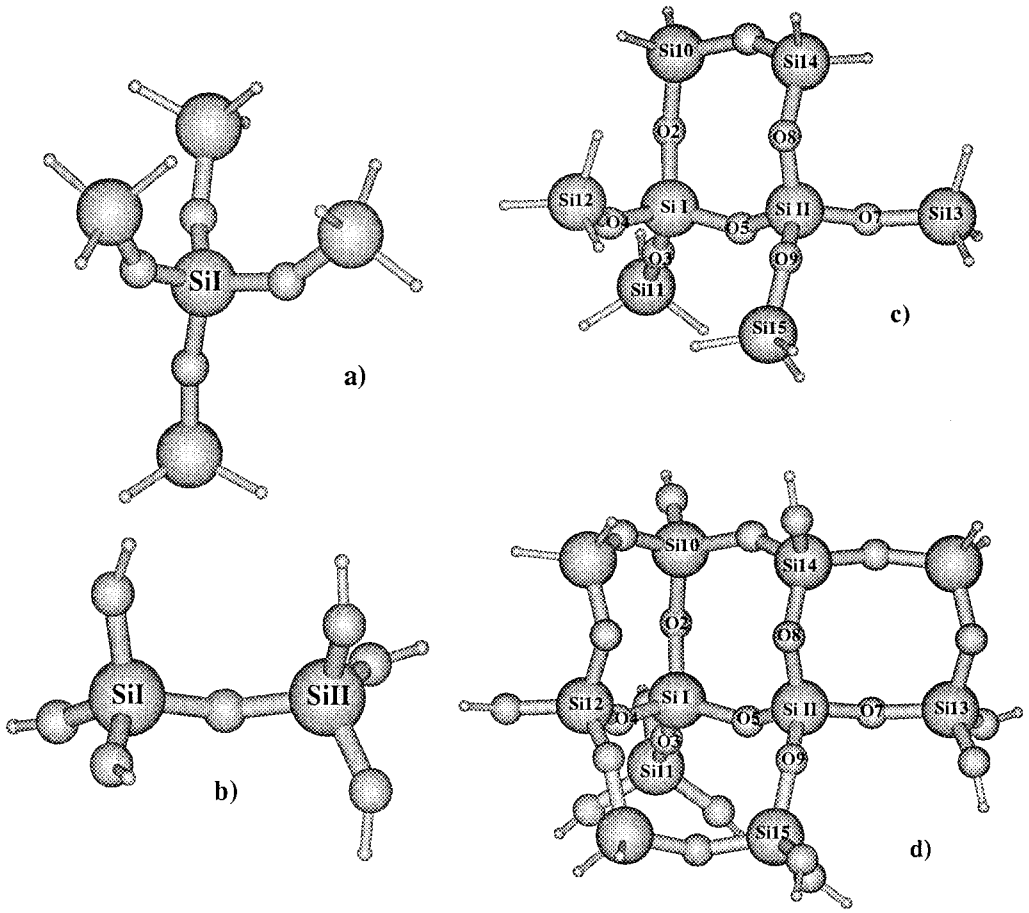

Figure 1. Typical cluster models of mazzite: (a) mSi_I or Si_{II}, (b) m1SiOSi, (c) m2SiOSi, (d) m3SiOSi.

samples with similar Si/Al ratios (Si/Al = 3.1;[15] Si/Al = 4.2[16,17]) rather than to the values obtained for a fully siliceous mazzite. These spectra correspond to silicon sites surrounded by a first shell of silicon neighbors. In the same spirit, we have compared the calculated ^{27}Al chemical shifts to experimental values obtained for a zeolite with Si/Al = 4.5.[18]

We have studied four types of model clusters in order to analyze the size effects on the calculated NMR properties (Figure 1). Three of these are two-site models, of the type $R_3Si_I-O-Si_{II}R_3$, where Si_I and Si_{II} are the two nonequivalent crystallographic sites in the framework of mazzite, and the other is a one-site model.

In all the clusters, the dangling bonds have been saturated with hydrogen atoms. The O−H bond distance has been set to 0.96 Å (if not optimized) and the Si−H bonds to 1.50 Å. In both cases, the H atoms have been positioned along the corresponding Si−O bonds in the mazzite experimental structure.

One-site clusters including two coordination spheres around the central silicon (Figure 1a) have been chosen to represent separately the two crystallographic sites (mSi_I and mSi_{II} models). The smaller of the three two-site clusters has the chemical formula $(OH)_3SiOSi(OH)_3$ and involves only the first coordination sphere around the Si_I-O-Si_{II} group. We will refer hereafter to this model as m1SiOSi (Figure 1b). A medium size two-site cluster was built adding a second coordination sphere around the Si_I-O−Si_{II} group, and is denoted as m2SiOSi (Figure 1c). According to the mazzite structure a four-membered ring appears, made by Si_I, Si_{II}, and two terminal silicon atoms linked by a bridging oxygen. Model clusters of this type have also been used to study the substitution of silicon by aluminum, with Al substituting Si in site I (m2AlOSi model) and in site II (m2SiOAl model), whereas a proton was used as a counterion and bound to the bridging AlOSi oxygen. Because of the nearly equal scattering powers of silicon and aluminum, X-ray diffraction cannot distinguish between these two nuclei yielding an average geometry. Hence, the aluminum location and its actual local geometry cannot be established experimentally. It is, however, well-known that Al−O bond lengths are longer than Si−O bonds and that AlOSi bond angles are in general smaller than the respective SiOSi angles. As we will describe in the next section, the geometry has been allowed to relax in order to take into account these differences between Si and Al. A larger two-site cluster has also been considered (Figure 1d), with three-atom coordination spheres and terminal OH groups. In this system, more four-membered rings appear breaking the symmetry of the Si_I and Si_{II} environments.

III. Theoretical Method

The calculations have been performed within the linear combination of Gaussian type orbitals-density functional formalism (LCGTO-DF),[19−21] using the deMon-KS and deMon-NMR programs.[13,22−24]

The geometry optimizations have been performed at the gradient-corrected density functional level using the Becke[25] functional for exchange and the Perdew[26] functional for correlation, hereafter designed as BP. The relaxation of the cluster structure has been allowed, keeping the terminal H atoms fixed (see section II). The intent is to allow the local geometry to relax, for example after the replacement of a Si with an Al, simulating with the fixed boundaries the constraints of the remaining zeolitic lattice, assumed to be rigid. The Al ion

dimension is not very different from that of Si (the Al−O bond distances in zeolites are about 0.1 Å longer than Si−O), and it was found that the relaxation following the Si → Al substitution is mainly a local phenomenon[27] implying that even relatively small clusters can give reliable geometries.

During the geometry optimization, all electron basis sets of DZP quality have been used for all heavy atoms whereas the terminal hydrogens have been described by a small DZ basis. In Huzinaga's notation the contraction patterns are (6321/521/1), (621/41/1) and (41) for Si and Al, O and H, respectively.[28] The associated auxiliary basis sets used to fit the density and the exchange-correlation potential are, for the same atoms, respectively (5,4;5,4), (5,2;5,2), and (5,1;5,1), where the usual deMon notation is used.[29] The fitting of the exchange-correlation potential has been performed using a grid of 26 angular × 64 radial points, whereas the energy and its gradient were evaluated using a more extended grid. As was pointed out by Malkin et al.,[13] more precise molecular orbital coefficients, necessary for NMR calculations, are obtained by performing one additional numerical SCF iteration using the enlarged grid.

The NMR shielding tensors have been calculated with the sum-over-states density functional perturbation theory (SOS-DFPT) in the LOC1 approximation,[13] along with the individual gauge for localized orbitals (IGLO) method, the occupied MOs being localized by the method of Foster and Boys.[30] For most of the NMR calculations, we used the IGLO-III basis set of Kutzelnigg et al.[31] for all the heavy atoms, keeping the standard (41) basis for the terminal H. Some calculations have also been carried out with the IGLO−II basis sets[31] or with mixed sets where only the central atoms of the clusters have been described with IGLO bases, while using standard basis sets for the peripheral atoms. The basis sets used will be hereafter named A (IgloIII on all heavy atoms, (41) on H); A′ (for the m3SiOSi model, IgloIII on the central (Si_IOSi_{II}) atoms and on the first and second coordination spheres; other atoms, Si (6321/521/1), O (621/41/1), H (41)); B (IgloII on all heavy atoms); C (IgloIII only on the central (Si_IOSi_{II}) atoms; other atoms, Si (6321/521/1), O (621/41/1), H (41)); D (IgloIII only on the central (Si_IOSi_{II}) atoms; other atoms, Si MCP + (311/211/1), O (621/41/1), H (41)).

In all cases, only the shielding tensors of the two central T atoms (T = Si, Al) were considered, because only these atoms have an appropriate local environment. Most of our shielding tensor calculations were performed using the PW91 functional.[32] Some calculations with other functionals are also reported, namely, BP (see above), PW86 (Perdew and Wang functional for exchange[33] and Perdew for correlation,[34] BLAP (Becke functional for exchange[25] associated with a laplacian correlation functional[35]).

IV. Results and Discussion

IV.1. ^{29}Si NMR for Two-Site Models of Increasing Size: $Si_2O_7H_6$, $Si_8O_8H_{16}$, $Si_{11}O_{24}H_{16}$. We first made some test calculations on the small two-site cluster model m1SiOSi which includes only the first oxygen shell around the silicons. To evaluate silicon chemical shifts (δ), which are directly comparable with experimental results, the ^{29}Si shielding tensor of tetramethylsilane (TMS) at its experimental structure was calculated, using IGLO basis sets on all atoms.

The results summarized in Table 1 show that, even for a small model such as $Si_2O_7H_6$, some qualitative characteristics of the ^{29}Si NMR spectrum of mazzite are already reproduced. The different geometrical environment of the two sites leads to two different calculated σ and δ values, following the same order as those known experimentally for mazzite,[15−17] i.e., Si_I at a more negative δ than Si_{II}.

TABLE 1. Shielding Constants and Chemical Shifts (in ppm) for $Si_2O_7H_6$ (IgloIII Bases, Experimental Structure from Reference 14)

functionals	σ (TMS)	σ, δ (Si_I)	σ, δ (Si_{II})	$\Delta(Si_{II}$-$Si_I)$
PW91	344.9	484.8, −139.9	462.5, −117.6	22.3
BP	339.8	479.5, −139.7	457.5, −117.7	22.0
PW86	330.0	473.4, −143.4	451.4, −121.4	22.0
BLAP3	334.5	484.6, −150.1	462.4, −127.9	22.2
exptl (δ)		−113.1[a]	−103.4[a]	9.7
		−112.0[b]	−103.4[b]	

[a] From ref 15 (cf. section II). [b] From ref 17 (cf. section II).

However, the shielding constant of both Si_I and Si_{II} are overestimated, and the difference between them, $\Delta(Si_{II} - Si_I) = 22$ ppm, is about twice the experimental value.

The dependence of the calculated NMR properties on the type of exchange and correlation functionals has been investigated using this model. The results, displayed in Table 1, show a considerable dependence of the absolute shielding constant on the functional. However, this dependence is lower for the δ values, except for the BLAP functional, and is completely negligible for the separation between the two signals. This demonstrates the stability of the method at least concerning the signal differences, which is very important if we want to use it for the assignment of NMR spectra.

The addition of one more coordination sphere (m2SiOSi model, Figure 1c) improves substantially the calculated chemical shifts (Table 2). The separation between the two signals is now very well reproduced. Moreover, both individual δ (Si_I) and δ (Si_{II}) values are very close to the experimental chemical shifts. We report in Table 2 the results obtained with the PW91 functional and the IGLO-III basis set, along with some other results obtained using different functionals and/or basis sets. As for the smaller m1SiOSi model, we observe a good stability of the chemical shifts and signal separations with respect to variations of the functional, despite a certain difference in the absolute shielding constants. The same situation occurs when comparing the results obtained with different basis sets and the same functional (PW91). Despite differences in σ values as large as 18 ppm, the δ and Δ values are within a few ppm even when mixed basis sets such as B and C are used (see the section "computational details" and Table 2 captions for details). We also notice that the results obtained with the more extended IGLO-III basis set are in better agreement with experiment than those obtained with IGLO−II. Again, the results obtained using the PW91 and BP functionals are almost identical and match better the experimental data. The results obtained for this model (m2SiOSi) with different basis sets show that substituting the IGLO bases on the noncentral atoms with the Si(6321/521/1) and O(621/41/1) bases (basis set C) leads to calculated δ values less negative with respect to those obtained using the IGLO bases on all heavy atoms. This could be due to the fact that those bases although less extended than the IGLO bases have nevertheless more diffuse s and p orbitals.

We also report in Table 2 the results obtained for the cluster $Si_{11}O_{24}H_{16}$ (m3SiOSi), including a third neighbor shell (oxygens). Two different basis sets, A′ and C, have been used. Despite the larger size of this cluster, the calculated chemical shifts are overestimated somewhat and the $\Delta(Si_{II} - Si_I)$ separation is worsened. In a subsequent section, we will try to explain the reasons for this behavior. It is quite evident from the data of Table 2 that we cannot attribute this result to a basis set effect. Two other factors are possible: (i) an effect of the

TABLE 2. Shielding Constants and Chemical Shifts (in ppm) for m2SiOSi and m3SiOSi Models[a]

functionals	models	basis	σ, δ (Si_I)	σ, δ (Si_{II})	$\Delta(Si_{II}-Si_I)$
PW91	m2SiOSi	A	458.2, −113.3	448.3, −103.4	9.9
BP		A	453.3, −113.5	443.2, −103.4	10.1
PW86		A	447.9, −117.9	438.0, −108.0	9.9
PW91		B	472.9, −108.7	464.2, −100.0	8.7
PW91		C	455.0, −110.1	446.9, −102.0	8.1
PW91		D	458.6, −113.7	449.3, −104.4	9.3
PW91	m3SiOSi	A′	468.0, −123.1	455.4, −110.5	12.6
PW91		C	466.0, −121.1	454.6, −109.7	11.4
	exptl (δ)		−113.1[b]	−103.4[b]	9.7
			−112.0[b]	−103.4[b]	

[a] Basis sets, A: IgloIII on all heavy atoms, H(41). A′: IgloIII on central (Si_I-O-Si_{II}) atoms and on the first and second coordination spheres. Other atoms: Si(6321/521/1), O(621/41/1), H(4,1). B: IgloII on all heavy atoms, H (41). C: IgloIII only on central (Si_I-O-Si_{II}). Other atoms: Si (6321/521/1), O (621/41/1), H (41). D: IgloIII on central (Si_I-O-Si_{II}) atoms. Other atoms: Si MCP + (311/211/1), O (621/41/1), H (41). $\delta_i = \sigma_{ref} - \sigma_i$; [ref = TMS PW91: σ(igloIII) = 344.9, σ(igloII) = 364.2. BP: σ(igloIII) = 339.8. PW86: σ(igloIII) = 330.0]. [b] From ref 15 (cf. section II). [c] From ref 17 (cf. section II).

cluster size and shape, with a fortuitous better agreement with experiment for the m2SiOSi model or (ii) an effect of the boundaries, i.e., a better representation of the zeolitic surroundings by SiH_3 than by $Si(OH)_3$ groups. Indeed, it has already been shown in the study of other properties, such as local softness[36] or zeolite−molecule interaction energies,[37] that OH terminal groups act artificially as electron donors via the semicovalent Si−O bonds. This effect would then lead to the overestimation of the Si shielding constants. The same tendency can be observed from a recent GIAO-HF study, where the calculated $\delta(^{29}Si)$ for α-quartz is shown to oscillate from less negative to more negative values when the last coordination shell incorporates terminal OH groups.[38]

When the geometry of the $Si_8O_8H_{16}$ cluster (m_2SiOSi) is fully optimized (fixing the H atoms), starting from the mazzite experimental structure, only minor distortions are found, so that the corresponding NMR parameters are practically unchanged with respect to those obtained for the experimental structure. This particularly good result is probably due to the rigidity of the mazzite framework and thus cannot be expected as well for other types of zeolites. In fact, studies of model clusters of the very flexible zeolite-β have shown that geometry optimization leads to a less accurate representation of its ^{29}Si NMR spectrum.[39] When available, we think it preferable to calculate the NMR properties using the experimental structure. However, there are no experimental data concerning the local aluminum environment and we are therefore obliged to use calculated equilibrium geometries. Since, for mazzite, the theoretical and experimental geometries of the m2SiOSi model are comparable, we can expect a good representation of the geometry when Si is substituted by Al. In fact, one may consider the calculated NMR properties as a test of the reliability of the calculated local structure around the aluminum.

IV.2. Si → Al substitution: ^{29}Si and ^{27}Al NMR. The two clusters $Si_7AlO_8H_{17}$ with Al in T_I and T_{II} sites, respectively, have been chosen to study the effects of the substitution of silicon by aluminum on the next Si site and to relate them to electronic and geometrical parameters. The excess negative charge arising from the Si → Al substitution has been compensated by a proton associated with the bridging oxygen O_b between T_I and T_{II}.

The optimized structural parameters, compared with their values in the fully siliceous model cluster, are presented in Table 3, whereas the corresponding shielding constants and chemical shifts are reported in Table 4. For both Si → Al substitutions, the main influence that aluminum exerts on the geometry of the neighboring silicon tetrahedron concerns the $Al-O_b-Si$ group. The hydrogen counterion on the bridging oxygen O_b gives rise to $Si-O_b$ and $Al-O_b$ bonds substantially longer with respect to the usual bonds that those atoms make with oxygen in aluminosilicates. The other Si−O bond lengths become slightly shorter (≅0.02 Å) which leads to almost no variation of the average Si−O bond length for both sites. The SiOSi bond angles change only by a few degrees; however, the average SiOT angles around T_I and T_{II} are slightly reduced with respect to the fully siliceous system, keeping roughly a 10° difference between the two sites. In fact, the trend that smaller angles correlate with smaller chemical shifts[11,39] also holds for Al substituted frameworks. However, the presence of Al at the next tetrahedron induces a much larger decrease of the chemical shift

TABLE 3. Calculated T−O Bond Distances (angstroms) and TOSi Bond Angles (degrees) (T = Si or Al) for $Si_7Al_8H_{16}$ (Al in Sites I and II) Compared with the Experimental Geometry for $Si_8O_8H_{16}$ (from ref 14)

	m2SiOSi (exptl)	$m2Si_IOAl$ (opt)	m2AlO Si_{II} (opt)
T_IO_2	1.658	1.622	1.719
O_3	1.641	1.615	1.705
O_4	1.654	1.616	1.704
O_5	1.654	1.731	1.931
$T_IO_2Si_{10}$	149.2	152.9	148.0
O_3Si_{11}	171.2	169.4	149.5
O_4Si_{12}	144.7	146.8	140.3
O_5Si_6	144.7	133.9	139.5
$T_{II}O_5$	1.631	1.921	1.702
O7	1.641	1.723	1.627
O_8	1.649	1.723	1.621
O_9	1.640	1.710	1.626
$T_{II}O_5Si_1$	144.7	133.9	139.5
O_7Si_{13}	146.5	137.7	143.5
O_8Si_{14}	137.3	133.6	140.9
O_9Si_{15}	136.6	132.5	136.0

TABLE 4. ^{29}Si and ^{27}Al Shielding Constants and Chemical Shifts (in ppm) for the m2SiOAl and m2AlOSi Models, Associated with Average TOSi Bond Angles and T−O Bond Distances (angstroms) (T = Si, Al)

	$m_2Si_IOSi_{II}$	$m_2Si_IOAl_{II}$	$m_2Al_IOSi_{II}$
$\sigma(T_I)$	458.2	453.5	505.7
$\delta(T_1)$	−113.3	−108.6	−99.3
	exptl −113.1[a]	exptl −107.1[c]	exptl ≅ −102.0[c]
	−112.0[b]		
$\langle T_I-O\rangle$	1.651	1.646	1.765
$\langle T_IOT\rangle$	152.5	150.8	144.3
$\sigma(T_{II})$	448.3	500.8	442.7
$\delta(T_{II})$	−103.4	−94.4	−97.8
	exptl −103.4[a,b]	exptl ≅ −94.0[c]	exptl −98.7[c]
$\langle T_{II}-O\rangle$	1.641	1.769	1.644
$\langle T_{II}OT\rangle$	141.3	134.4	140.0

[a] From ref 15 (cf. section II). [b] From ref 17 (cf. section II). [c] From ref 18 (cf. section II).

TABLE 5. Electronic Properties Calculated for the Mazzite Models

site I	mSi_I	$m2Si_IOSi$	$\langle Si_I = \langle Si_{II}$	m_3Si_IOSi	m_2Si_IOAl	m_2Al_IOSi
σ[a]	454.1	458.2	458.2	468.0	453.5	505.7
$\langle TOT_i \rangle$	152.5	152.5	152.5	152.5	150.8	144.3
q(T)[b]	1.15	1.09	1.09	1.06	1.24	1.37
M(T)[c]	4.130	4.183	4.186	4.172	4.158	2.760
$\langle q(O) \rangle$[b]	−0.55	−0.55	−0.55	−0.56	−0.61	−0.72
$\langle M(T-O) \rangle$[c]	0.959	0.966	0.966	0.965	0.962	0.627
E_{1s}(T)[d]	−65.2345	−65.2387	−65.2401	−65.2231	−65.2552	−55.1191
site II	mSi_{II}	$m2SiOSi_{II}$	$\langle Si_{II} = \langle Si_I$	m_3SiOSi_{II}	m_2SiOAl_{II}	m_2AlOSi_{II}
σ[a]	445.1	448.3	457.6	455.4	500.8	442.7
$\langle TOT_i \rangle$	141.3	141.3	152.5	141.3	134.4	140.0
q(T)[b]	1.23	1.26	1.13	1.34	1.35	1.30
M(T)[c]	4.086	4.009	4.081	3.851	2.711	3.996
$\langle q(O) \rangle$[b]	−0.59	−0.60	−0.56	−0.62	−0.75	−0.64
$\langle M(T-O) \rangle$[c]	0.947	0.931	0.949	0.918	0.616	0.933
E_{1s}(T)[d]	−65.2247	−65.2294	−65.2321	−65.2099	−55.1180	−65.2504

[a] In ppm. [b] Mulliken charge on the atom T or average charge on the surrounding oxygens. [c] Mayer bond orders: M(T) is the valence of T, M(T−O) the average T−O bond order. [d] Energy of the 1s orbital in hartrees.

than expected from the small decrease of the average SiOT angle: the calculated ^{29}Si shielding constants are indeed reduced by about 5 ppm, the value also given by a known empirical rule,[40] and corroborated by several experimental measurements.[17,18,41] Larger structural changes affect the aluminum tetrahedron. The Al−O bond lengths are about 1.7 Å except for the longer Al−O_b bond at 1.9 Å, and the AlOSi bond angles are substantially reduced. In particular, the very large Si_IOSi_{II} angle of 171° is reduced to 149° after the $Si_I \rightarrow Al_I$ substitution.

The ^{27}Al shielding constants of the two sites were also calculated at their optimized geometries. The order and separation of the two signals are well reproduced. It is found experimentally[18] that aluminum at the T_I and T_{II} sites of mazzite yields two signals in the range 55−65 ppm with $\delta(Al_1) < \delta(Al_2)$ and thus $\sigma(Al_1) > \sigma(Al_2)$, as obtained from our calculated σ values (Table 4). The usual external reference for the ^{27}Al NMR spectra is $Al(H_2O)^{3+}_6$ corresponding to $Al(NO_3)_3$ in aqueous solution. To evaluate ^{27}Al chemical shifts, we optimized the structure of an isolated T_h $Al(H_2O)^{3+}_6$ ion with the water molecules arranged in an octahedral-like geometry. The calculated shielding constant for aluminum in this ion, using the IGLO III basis set, is 575.4 ppm. The ^{27}Al chemical shifts evaluated with such a reference are 69.7 (Al_I) and 74.6 (Al_{II}) vs 54 and 62 ppm from experimental NMR spectra. The agreement is qualitatively good but with an absolute error of about 13−15 ppm. We attributed this error to the too simple representation of the reference complex (lack of solvation, counterions, etc.). To verify this hypothesis, we calculated the shielding constant of trimethylaluminum (TMA) and evaluated its chemical shift with respect to $Al(H_2O)_6^{3+}$. We actually obtained two very different values for TMA as a monomer or as a dimer. The monomer corresponds to a calculated δ value of 332.6 ppm (σ = 242.8), which is very far from the experimental value of 156 ppm.[42] However, TMA is known to form a stable dimer complex and the calculation of the dimer chemical shift yields a value of 169 ppm (σ = 406.4). The error corresponding to the evaluation of the chemical shift of TMA with respect to our model for $Al(H_2O)_6^{3+}$ (13 ppm) is thus similar to the error we found for the mazzite models, supporting our previous hypothesis. To avoid this difficulty, we present the ^{27}Al chemical shifts with respect to TMA, for both experimental and theoretical data, obtaining a quite good agreement, as shown in Table 4. The downfield shift of both Si sites with one next neighbor Al is very well reproduced by the calculation, with an absolute error of less than 1.5 ppm, whereas the maximum error for δ (^{27}Al) is less than 3 ppm. It is worth noting that, due to their broadness, ^{27}Al NMR signals cannot be determined with an accuracy greater than about 2 ppm.[18] These results prove, a posteriori, the validity of the calculated relaxation following the Si → Al substitution.

V. Effect of Geometrical and Electronic factors on the ^{29}Si Chemical Shift

Experimental NMR spectra show that ^{29}Si chemical shifts in zeolites are dependent on the local geometry around the site for a given chemical environment and also on the number of Al atoms in the next coordination shells.[1−5] The fact that, in a fully siliceous solid, crystallographically different silicons have different chemical shifts demonstrates that small geometrical changes induce variations on the electronic structure which are large enough to modify significantly the silicon shielding tensors.

It was already shown, in the case of zeolite-β,[39] that the main geometrical parameters, in this context, are the SiOSi angles, whereas the Si−O bond lengths have a much smaller influence. The substitution of Si by Al in the m2SiOSi model induces only a small decrease of the average SiOT angle around the neighboring silicons, namely, 1.7° for Si_I ($m2Si_IOAl$) and 1.3° for Si_{II} ($m2AlOSi_{II}$). This variation is not sufficient to explain the downfield shifts observed for both sites and reproduced by the calculations (Table 4).

It is therefore clear that an additional electronic effect occurs in this case. In the same way, electronic effects are also directly responsible for the variation of σ (Si_I) and σ (Si_{II}) on going from the mSi to the m2SiOSi and m3SiOSi models.

To determine typical differences between the two nonequivalent sites, or, for the same site, between different environments and then to find out a possible correlation with the screening constants, we have compared several electronic characteristics of the models (Table 5). These characterize the T atoms (Mulliken charge, q, valence, M, and 1s orbital energy) and also the four surrounding oxygens (average values of their Mulliken charges and T−O Mayer bond orders[43]).

To analyze in more detail the effect of the TOT bond angles, we have modified the m2Si OSi cluster, giving to Si_{II} the same SiOSi angles as those of Si_I, keeping the other internal coordinates constant. As shown in Table 5 ($\langle Si_I = \langle Si_{II}$ column), the calculated σ (Si_{II}) value becomes almost equal to σ (Si_I). In the same time, all the electronic properties reported for the $Si_{II}O_4$ group become very similar to those of the Si_IO4 entity. We can thus conclude that, within the same model, i.e., with

TABLE 6. Shielding Constants (σ) and Chemical Shifts (δ) (in ppm) for Si_A in $H_3Si_A-O_b-Si_pR_3$ with R = H, OH, and OSiH3, Compared with the Main LMO Contributions to σ

		LMO					
R	σ, δ (Si_A)	core (Si_A)	(Si_A−H)3	Si_A-O_b	LP(O_b)[a]	O_b-Si_p	Σ[b]
H	386.0, −41.1	789.4	−331.1	−84.3	17.0	−3.7	387.3
OH	392.9, −48.0	790.9	−329.3	−81.4	18.3	−5.3	393.2
$OSiH_3$	385.7, −40.8	792.2	−338.3	−84.0	18.6	−3.0	385.5

[a] Lone pair contribution. [b] Sum of all listed contributions.

comparable environments, the SiOSi bond angles are the main factors governing the ^{29}Si NMR chemical shift. Moreover, for the fully siliceous models, mSi, m2SiOSi, and m3SiOSi, there is an unambiguous correlation between the σ values and the electronic parameters of each site: Si_I is more screened (higher σ value) than Si_{II}, and correspondingly, it has a less positive Mulliken charge, larger valence, and Si−O bond order values and more contracted core orbitals (only 1s Si eigenvalues are reported here, but the same trend holds for 2s and 2p orbitals).

The variation of the oxygen Mulliken charges with the geometry, i.e., with the ⟨SiOSi⟩ angle, is much smaller than that of silicon. However, its behavior follows the expected trend that a more negative O charge is associated with less electron density on Si and in the Si−O bonds and corresponds to a smaller ⟨SiOSi⟩ angle.[44] The comparison of the two models including an Al atom (m2SiOAl and m2AlOSi) shows that again, the element in T_I (larger ⟨TOT⟩ angle), when compared to the same element in T_{II}, has a larger screening constant. The corresponding electronic parameters vary from Si_I to Si_{II} according to the same trend as described above for the fully siliceous models. However, their variation from Al_I to Al_{II} is almost insignificant despite a difference of 10° between their average ⟨AlOSi⟩ angles.

On the other hand, it is not possible to find a satisfactory quantitative explanation of the increase of $\sigma(Si_I)$ and $\sigma(Si_{II})$ in terms of the electronic parameters of Table 5, comparing the models of different size, mSi, m2SiOSi, and m3SiOSi. Similarly, it is not possible to rationalize the evolution of σ (Si) upon introduction of an aluminum in the m2SiOSi cluster. The presence of Al decreases the electronic population of the neighboring silicon, but the variation of the charge on Si_I (from +1.09 to +1.24) and on Si_{II} (from +1.26 to +1.30) while showing coherent trends are not quantitatively consistent with the corresponding variation of the screening constants ($\Delta\sigma(Si_I) = -4.7$ and $\Delta\sigma(Si_{II}) = -5.6$). The other parameters behave in a similar fashion.

To get more insight into the electronic effects related to the size of the cluster, we have considered in more detail the evolution of the screening constant of Si_A in the three simple models $H_3Si_A-O_b-Si_pR_3$, with R = H, OH, and $OSiH_3$.

We have reported, in Table 6, the σ (Si_A) values calculated for these 3 models and their decomposition into contributions from the individual localized molecular orbitals (LMO). The main contributions arise from the core orbitals of Si_A (1s, 2s, 2p), the Si_A-H, Si_A-O_b, O_b-Si_p bonds and the O_b lone pair (LP). The sum (Σ) of all these terms is very similar to the corresponding σ values, showing that other contributions are negligible.

The shielding constants calculated for R = H and R = $OSiH_3$ are equivalent. In contrast, the presence of terminal OH groups increases this value by 7 ppm, which indicates a substantial electron donation to Si_A. The analysis of Table 6 does not provide a simple explanation for that result. Indeed, although R = H and R = $OSiH_3$ lead to similar screening constants for Si_A, their LMO contributions are quite different and it seems difficult to assess whether terminal hydrogens behave like longer silicate linkages. However, it is worth noting that, for the three clusters, the dominant contribution is due to Si_AH_3 and that this contribution is too positive (less negative Si_A-H term) when R = OH is present instead of $OSiH_3$, which correlates with an overestimated screening.

TABLE 7. Calculated Shielding Constants (σ) and Their LMO Contributions for ^{29}Si at Sites I and II of the Different Models

site	LMO[a]	mSi[b]	m_2SiOSi	m_3SiOSi	m_2SiAl[c]
site I	core	820.8	819.9	819.8	816.6
	$Si_I-O_2-Si_{10}$	−90.6	−88.1	−87.8	−97.0
	$Si_I-O_3-Si_{11}$	−90.0	−91.3	−84.5	−92.2
	$Si_I-O_4-Si_{12}$	−91.1	−91.9	−90.2	−98.9
	$Si_I-O_5-Si_{II}$	−91.6	−88.5	−90.7	−73.3
	Σ	457.5	460.1	466.6	455.2
	σ	454.1	458.2	468.0	453.5
site II	core	822.1	821.1	818.4	819.3
	$Si_{II}-O_5-Si_I$	−94.3	−90.2	−90.2	−75.9
	$Si_{II}-O_7-Si_{13}$	−91.9	−93.2	−89.4	−95.8
	$Si_{II}-O_8-Si_{14}$	−93.4	−92.5	−90.9	−101.0
	$Si_{II}-O_9-Si_{15}$	−95.5	−96.0	−93.7	−102.4
	Σ	447.0	449.2	454.2	444.2
	σ	445.1	448.3	455.4	442.7

[a] Contributions of the localized molecular orbitals to σ. $Si_I(Si_{II})-O_x-Si_y$ refer to contributions of molecular orbitals localized in the atoms $Si_I(Si_{II})$, O_x and Si_y. Σ corresponds to the sum of the listed contributions. [b] mSi denotes mSi_I and mSi_{II}. [c] m_2SiAl denotes $m_2Si_IOAl_{II}$ and $m_2Al_IOSi_{II}$.

We have found it interesting to apply the same kind of analysis to $\sigma(Si_I)$ and $\sigma(Si_{II})$, comparing all the mazzite models. Five contributions to σ have been considered: that corresponding to the Si_I (Si_{II}) core orbitals and, for each of the four linkages $Si_{I(II)}-O_x-T_y$, a global value, comprehensive of the contributions from the $Si_{I(II)}-O_x$ and O_x-T_y bonds and from the O_x lone pairs.

These results are presented in Table 7. For clarity, the Si and O atoms are labeled as in Table 3 and Figure 1. The difference of about 10 ppm calculated for all the clusters between $\sigma(Si_I)$ and $\sigma(Si_{II})$ comes essentially from the paramagnetic bond contributions, directly related to the local geometry and in particular to the different bond angles.

The small difference in the core contributions (1.2 ppm for the fully siliceous models) comes from the $n = 2$ shell, slightly affected by the local environment, whereas the 1s contribution to σ is constant in all the clusters studied.

As already reported for zeolite-β,[39] the one-site models provide a good description of the peak separation ($\Delta\delta = 9$ instead of 9.7 ppm, experimentally), although an upfield shift is obtained for both sites, which amounts to 3−4 ppm with respect to the δ values calculated for the m2SiOSi model. As seen from Table 7, mSi_I and mSi_{II} have, each, four comparable paramagnetic contributions, in contrast with m2SiOSi where the linkages contained in the four-membered ring (through O_2, O_5, O_8) provide significantly more positive contributions to $\sigma(Si_I)$ and $\sigma(Si_{II})$. This shows that σ (δ) does not depend only on the

TOT angle (and T−O bond) values, but also on the connectivity of the silicate structure, with the trend that a silicon atom included in a 4-m ring will have a larger shielding constant, keeping all other variables equal (TOT angles and number of neighboring Al). Since Si_I and Si_{II} belong to the same 4-m ring, the error made in using the one-site models is comparable for each site. This leads to a good description of the peak separation, despite of slightly underestimated shielding constants.

The analysis of the LMO contributions to σ (Si_I) for m2SiOSi shows a clear influence of the cluster size and shape: the 3.4 ppm difference between the Si_I-O_4−Si_{12} and Si_I-O_5−Si_{II} contributions should not exist, because O_4 and O_5 are equivalent in the solid.

In fact, these two contributions are found to be equivalent in the mSi(I) and m3SiOSi models. In the first case, there is no 4-m ring, whereas in m3SiOSi, the two linkages are both included in a 4-m ring. We could thus conclude that m3SiOSi would lead to a better description of δ(Si). However, its calculated screening constants are overestimated with respect to the experimental values and in poorer agreement than those obtained with m2SiOSi. We see, from Table 7, that the overestimation of $\sigma(Si_I)$ is related to a strong decrease of the paramagnetic contribution from the $Si_I-O_3-Si_{11}$ linkage, that we attribute to the presence of three OH terminal groups on Si_{11}. Indeed, its contribution to σ is 6.8 ppm more positive than that calculated for m2SiOSi with a SiH_3 terminal group, and this amount is roughly equal to the difference in $\sigma(Si_I)$ between the two cluster models. A similar effect also exists for $\sigma(Si_{II})$ due to the $Si_{II}-O_7-Si_{13}$ and $Si_{II}-O_9-Si_{15}$ linkages bearing two terminal OH groups on Si_{13} and Si_{15}, respectively, leading again to underestimated paramagnetic contributions.

These considerations indicate that, to overcome the size and shape limitations of a relatively small cluster like m2SiOSi, it is not sufficient to simply add a coordination shell, because the terminal OH groups left after the ring closure can affect the results much more than the size effects.

Introducing an Al atom in T_{II} and T_I (m2SiAl column of Table 7) induces a decrease of about 5 ppm of the shielding constant of the neighboring silicon. The LMO analysis shows that it is due, partly, to the core contributions (2s and 2p orbitals) and partly to the paramagnetic terms. There is a strong decrease of the $Si-O_5-Al$ contributions, when Al is in site I or site II, which reflects the important elongations of the $Si-O_5$ and $Al-O_5$ bonds. However, this decrease is partly compensated by the increase of the three other contributions, leading to a final decrease of about 5 ppm for σ (Si_I) and σ (Si_{II}).

VI. Conclusion

The ^{29}Si and ^{27}Al NMR chemical shifts of the zeolite mazzite have been calculated using the SOS-DFPT method. We have analyzed the effects of the cluster size, basis set extension and choice of the approximate exchange and correlation functionals on the calculated chemical shifts of ^{29}Si at sites I and II. We have shown that a good description of the relative position of the NMR peaks is obtained using clusters including two coordination shells around each site. The description of the absolute values of ^{29}Si and ^{27}Al chemical shifts has been obtained using a two-site model, fulfilling the above condition and containing a four-membered ring between the two sites and terminal SiH_3 groups. The calculated screening constants of the two sites show an unambiguous correlation with the average $\langle T_IOSi\rangle$ and $\langle T_{II}OSi\rangle$ bond angles, larger screening constants (more negative δ) being associated with larger bond angles for both ^{29}Si and ^{27}Al.

The NMR chemical shifts correlate with the local geometry through the electronic characteristics of the system. The analysis of the calculated electronic properties shows that it is possible to rationalize the ordering of the chemical shifts of different sites when they are represented by the same type of cluster. In this case, a larger screening constant characterizes a T atom with more electron density and more strongly bonded to surrounding oxygens (bearing smaller charge), which correlates with globally larger bond angles. However, the calculated electronic properties of a cluster are dependent on its size and shape. Hence, one cannot easily correlate NMR chemical shifts and electronic properties for zeolites with different structures and compositions.

Finally, the analysis of the orbital contributions to the ^{29}Si screening constants has underlined the role of the shape of the system, i.e., the importance to take into account the connectivity of the T−O bonding, independently of the bond length and bond angle values.

Acknowledgment. Financial assistance from IFCPAR (Project 1206-1) is gratefully acknowledged. Calculations were partially performed on the NEC-SX4 at CSCS Manno (Switzerland).

References and Notes

(1) Fyfe, C. A.; Gobbi, G. C.; Klinowski, J.; Thomas, J. M.; Ramdas, S. *Nature* **1982**, *296*, 530.
(2) Fyfe, C. A.; O'Brien, J. H.; Strobl, H. *Nature* **1987**, *326*, 281.
(3) Engelhardt, G.; Lohse, U.; Lippmaa, E.; Tarmak, M.; Mägi, M. Z. *Anorg. Allg. Chem.* **1981**, *482*, 49.
(4) Klinowski, J.; Ramdas, S.; Thomas, J. M.; Fyfe, C. A.; Hartman, J. S. *J. Chem. Soc., Faraday Trans.* **1982**, *78*, 1025.
(5) Melchior, M. T.; Vaughan, D. E. W..; Jacobson, A. J. *J. Am. Chem. Soc.* **1982**, *104*, 4859.
(6) Thomas, J. M.; Fyfe, C. A.; Ramdas, S.; Klinowski, J.; Gobbi, G. C. *J. Phys. Chem.* **1982**, *86*, 3061.
(7) Ramdas, S.; Klinowski, J. *Nature* **1984**, *308*, 521.
(8) Himei, H.; Yamada, M.; Oumi, Y.; Kubo, M.; Stirling, A.; Vetrivel, R.; Broklawik, E.; Miyamoto, A. *Microporous Mater.* **1996**, *7*, 235.
(9) Fyfe, C. A.; Strobl, H; Kokotailo, G. T.; Pasztor, C. T.; Barlow, G. E.; Bradley, S. *Zeolite* **1988**, *8*, 132.
(10) Fyfe, C. A.; Grondey, H.; Feng, Y.; Kokotailo, G. T. *J. Am. Chem. Soc.* **1990**, *112*, 8812.
(11) Weller, M. T.; Dann, S. E.; Johnson, G. M.; Mead, P. J. In *Progress in Zeolite and Microporous Materials*; Chon, H., Ihm, S. K., Uh, Y. S., Eds.; Studies in surface Science and Catalysis: Elsevier Science B. V. New York, Vol. 105 1997; 455.
(12) Radeglia, R.; Engelhardt, G. *Chem. Phys. Lett.* **1985**, *114*, 28.
(13) Malkin, V. G.; Malkina, O. L.; Casida, M. E.; Salahub, D. R. *J. Am. Chem. Soc.* **1994**, *116*, 5898.
(14) Galli, E. Cryst. *Struct. Commun.* **1974**, *3*, 339.
(15) Siedle, A. R.; Newmark, R. A. *J. Am. Chem. Soc.* **1981**, *103*, 1240.
(16) Michel, M.; Meiler, W.; Pfeifer, H. *J. Mol. Catal.* **1976**, *1*, 85.
(17) Fyfe, C. A.; Gobbi, G. C.; Kennedy, G. J.; Graham, J. D.; Osubko, R. S.; Murphy, W. J.; Bothner-By, A.; Meiler, J.; Chesnick, A. S. *Zeolites* **1985**, *5*, 179.
(18) Chauvin, B.; Massiani, P.; Dutartre, R.; Figuéras, F.; Fajula, F.; Des Courières, T. *Zeolites* **1990**, *10*, 174.
(19) Sambe, H.; Felton, R. H. *J. Chem. Phys.* **1975**, *62*, 1122.
(20) Dunlap, B. I.; Conolly, J. W. D.; Sabin, J. R. *J. Chem. Phys.* **1979**, *71*, 3396.
(21) Salahub, D. R. *Adv. Chem. Phys.* **1987**, *69*, 447.
(22) St-Amant, A.; Salahub, D. R. *Chem. Phys. Lett.* **1990**, *169*, 387.
(23) St-Amant, A. Ph.D. Thesis, Université de Montréal 1992.
(24) Casida, M. E.; Daul, C. D.; Goursot, A.; Koester, A.; Petterson, L.; Proynov, E.; St-Amant, A.; Salahub, D. R.; Duarte, H.; Godbout, N.; Guan, J.; Jamorski, C.; Lebouf, M.; Malkin, V.; Malkina, O.; Sim, F.; Vela, A. *deMon Software−deMon-KS3 Module*, University of Montreal: Montreal, 1996.
(25) Becke, A. D. *Phys. Rev. A* **1988**, *38*, 3098.
(26) Perdew, J. P. *Phys. Rev. B* **1986**, *33*, 8822.
(27) Kramer, G. J.; de Man, A. J. M.; van Santen, R. A. *J. Am. Chem. Soc.* **1991**, *113*, 6435.
(28) Godbout, N.; Salahub, D. R.; Andzelm, J.; Wimmer, E. *Can. J. Chem.* **1992**, *70*, 560.
(29) Papài, I.; Goursot, A.; Fajula, F.; Weber, J. *J. Phys. Chem.* **1994**, *98*, 4654.

(30) Foster, S.; Boys, S. F. *Rev. Mod. Phys.* **1960**, *32*, 303.
(31) Kutzelnigg, W.; Fleischer, U.; Schindler, M. In *NMR-Basic Principles and Progress*: Springer-Verlag: Heidelberg, 1990; Vol. 23, p 165.
(32) Perdew, J. P.; Wang, Y. *Phys. Rev. B* **1992**, *45*, 13244. Perdew, J. P.; Chevary, J. A.; Vosko, S. H.; Jackson, K. A.; Pederson, M. R.; Singh, D. J.; Fiolhais, C. *Phys. Rev. B* **1992**, *46*, 6671.
(33) Perdew, J. P.; Wang, Y. *Phys. Rev. B.* **1986**, *33*, 8800.
(34) Perdew, J. P. *Phys. Rev. B.* **1986**, *33*, 8822; *Phys. Rev. B.* **1986**, *34*, 7406 (erratum).
(35) Proynov, E. I.; Ruiz, E.; Vela, A.; Salahub, D. R. *Int. J. Quantum Chem.* **1995**, *29*, 61. Proynov, E. I.; Sirois, S.; Salahub, D. R. *Int. J. Quantum Chem.* **1997**, *64*, 427.
(36) Krishnamurty, S.; Vetrivel, R.; Pal, S. To be published.
(37) Blaszkowski, S. R.; Van Santen, R. A. *J. Phys. Chem.* **1995**, *99*, 11728.
(38) Bussemer, B.; Schröder, K. P.; Sauer, J. *Solid State Nucl. Magn. Res.* **1997**, *9*, 155.
(39) Valerio, G.; Goursot, A.; Vetrivel, R.; Malkina, O.; Malkin, V.; Salahub, D. R. *J. Am. Chem. Soc*. To be published.
(40) Engelhardt, G.; Michel, D. *High-Resolution Solid-State NMR of Silicates and Zeolites*; Wiley: Chichester, 1987.
(41) Massiani, P.; Fajula, F.; Di Renzo, F. *J. Chem. Soc., Chem. Commun.* 1988, 814.
(42) Mason, J. *Multinuclear NMR*: Plenum Press: New York, 1987.
(43) Mayer, I. *Chem. Phys. Lett.* **1983**, *97*, 270
(44) Goursot, A.; Fajula, F.; Daul, C.; Weber, J. *J. Phys. Chem.* **1988**, *92*, 4456.